Small Galaxy Groups
ASP Conference Series, Vol. 209, 2000
M. Valtonen and C. Flynn, eds.

Mass-to-Light Ratio Measurements of Galaxies, Groups, and Clusters using the Numerical Action Method

Ed Shaya

RITSS/NASA

P. J. E. Peebles & Steven Phelps

Princeton University

R. Brent Tully

IfA/University of Hawaii

Abstract. The numerical action variational method (NAM) is an elegant, non-chaotic technique for calculating the trajectories of gravitating systems in a cosmological context. It has been used extensively for establishing orbits of Local Group galaxies in a series of papers (Peebles 1989, 1990, 1994, 1995) and for the Local Supercluster (Shaya, Peebles, & Tully 1995).

Our repertoir of tools include code that holds present distances constant and predicts possible redshifts, one that holds present redshifts constant and predicts possible distances, and one that varies masses of each mass tracer and simultaneously satisfies both distance and redshift.

Our results indicate a $\Omega_0 = 0.2$, a mass-to-light ratio of field galaxies in the range of 100 $M_\odot/L_\odot$ in blue light ($t_0 = 11$ Gyr with no cosmological constant), but for the Virgo Cluster, the value is 6 or 7 times higher. The higher values of Ω_0 determined from using the IRAS galaxy distributions may be a result of under weighting this important mass component of the universe plus a poor correlation between cluster and field galaxy distributions.

1. Introduction

If peculiar velocities were generated by the unbalancing of gravitational forces due to the clustering of matter, then a map of the peculiar velocities provides a measure of the mass distribution in the universe. In fact, the only observed manifestation of dark matter, so far, is its collective gravitational effect which is represented in peculiar velocities and rotation speeds. Our collaboration has made a three pronged attack to solve the celestial mechanics problem of nearby galaxies: (i) the variational Numerical Action Method (NAM) allows orbits to be traced back in time from the present even for regions where the present interactions are strongly non-linear, (ii) the extended Nearby Galaxy Catalog, incorporating both optical and IRAS redshift survey information, provides the

highest resolution map of the distribution of nearby matter currently in use, and (iii) distance estimates obtained by Tully and collaborators are combined with those available in the literature to provide high quality distances throughout the Local Supercluster region.

If the mass density fluctuations are modest, $\delta_m \leq 1$, then the relationship between peculiar velocities, $\mathbf{v}$, and the *observed* galaxy fluctuation field, δ_g, is (Peebles 1980):

$$\mathbf{v} = \frac{\beta}{4\pi} \int d^3\mathbf{r}' \frac{\delta_g(\mathbf{r}')(\mathbf{r}' - \mathbf{r})}{|\mathbf{r}' - \mathbf{r}|^3} \tag{1}$$

where $\beta = \Omega_0^{0.6}/b$ and $b = \delta_g/\delta_m$, the bias parameter (Kaiser 1984), defines the relationship between the observable galaxy distribution and the mass distribution.

One of the general approaches to the problem takes direct recourse to Eq. (1). For a given β, velocities are *predicted* by the right side of Eq. (1) and can be compared with *observed* velocities for galaxies with distance determinations. Shaya, Tully, & Pierce (1992) used this method and found the value $\beta_O \lesssim 0.25$, where the subscript O indicates use of an optical catalog.

Linear theory is only accurate on scales of ~ 20 Mpc and larger because it is only on those scales that $\delta_g \ll 1$ is strictly valid. This means that the methods using linear theory must smooth over small scales and therefore important details are overlooked. One such detail is that the morphological type of the galaxies and/or the fraction of galaxies in clusters may change drastically between smoothed resolution elements. Comparison of derived mass density fields with galaxy number counts are naive when such details are ignored. Secondly, one is forced to go out to great distances to provide a sufficient number of resolution elements. At great distances, measurements of peculiar motion are poor because distance errors masquerade as peculiar motions. The remedy is to use fully non-linear NAM to relate observed positions and velocities to masses.

2. The Numerical Action Method (NAM)

It is not possible to use an N-body code to calculate the motions of galaxies backward in time because one does not know all six coordinates of phase space for galaxies at a specific instant, and because the problem is chaotic in that small errors grow exponentially with time. We know three elements of the present phase-space distribution of galaxies very accurately; two coordinates of projection on the sky and radial velocities. Peebles (1989, 1990, 1994, 1995) described a variational principle (action) method to calculate trajectories based on a substitution of the three missing elements of phase-space with an equal number of constraints on initial conditions. The method involves finding the paths that result in extrema of variation of the time integral of the Lagrangian in expanding coordinates.

$$\delta S = \delta \int_0^{t_0} dt [\sum_N K_i - \sum_N V_i - V_b] \tag{2}$$

https://doi.org/10.1017/S0252921100055433 Published online by Cambridge University Press

where K_i and V_i are the kinematic and potential energies of the N individual mass components and V_b is the background potential. The early time constraints on the variation are

$$a^2 d\mathbf{x}_i/dt \to 0 \text{ as } a \to 0 \tag{3}$$

where a is the normalized scale size of the universe. Thus, the constraint on initial peculiar velocities is simply that they were not extremely large at early times. In other words, present-day motions that deviate from general expansion have grown gradually from gravitational perturbations. A corollary of the gradual growth in random motions is that one does not have to calculate too far backward in time to account for nearly all of the peculiar velocities. It is not necessary, in the numerical integration, to have many time steps before $z = 3$ to reasonably follow the development of observed peculiar velocities.

The description of orbits no longer requires a functional form as it did in our earlier works. Peebles (1995) has recast the action integral so that the position of any particle is completely free at each time step. Arbitrarily sharp turns and accelerations are now allowed.

A check on the calculation can be made by running an N-body program forward starting at the earliest time step of the action analysis. We routinely make this check to test that we are taking small enough time steps and using enough coefficients to describe the paths. Most orbits are accurately reproduced. This agreement between action and N-body orbits has also been demonstrated by Branchini & Carlberg (1994). The methodology has also been explored by Giavalisco et al. (1993) and Dunn & Laflamme (1993, 1995). It has been shown that the action procedure works, with three significant caveats. First, on the observational side, one must have an adequate galaxy catalog. Second, if the orbits of bodies have crossed (completed $\gtrsim$ a half orbit) then there are multiple solutions. Third, matter must be distributed in a closely correlated fashion with the light tracers. Thus, the NAM calculations are testing the mass–light correlation and the χ^2 goodness of fit to observed distances is an indicator of the amplitude of this correlation.

Recently, Peebles and Phelps (1999) have developed a numerical variational principle in which the angular position in the sky and the radial velocity were the direct inputs to the computation of orbits. A given numerical solution to the variational condition for the orbits of the mass tracers is a self-consistent model for the evolution of the mass distribution. This model contains the predicted present distances of each of the mass tracers. Some of these entities have measured distances. We use the scatter between measured and predicted distances to discriminate among solutions based on different cosmological parameters.

There are multiplicity of solutions. Some of these arise because of the famous triple value regions around massive objects, in which there are three locations along a line of sight that have the same redshift. Other solutions arise because there are sometimes several possible initial configurations that result in the present configuration. These possibilities are found by making many runs of the code using random initial guesses for the trajectories of the mass tracers.

3. Results

3.1. 3000 km s^{-1} radius

Figure 1 provides an example of our χ^2 contour maps. The axes are the two free parameters: M/L and t_0. Orbits are computed for 1323 elements within 3000 km s^{-1} and the large-scale structure beyond 3000 km s^{-1} has been represented by the Lauer & Postman (1994) rich cluster sample. Contour levels are spaced at roughly 1σ intervals. Dotted curves are loci of constant H_0 and dot-dash curves are loci of constant Ω_0.

The influence of the tidal field beyond 3000 km s^{-1} provides a small improvement to the reduced χ^2. The geometry of the nearby superclusters is such that it provides a compression between our position and most of the Local Supercluster. The consequence is that slightly less mass is required at a given value for t_0 to develop observed peculiar velocities. Although the influence of structure beyond 3000 km s^{-1} is minor on the χ^2 fits of the local sample, there are very large differences in streaming patterns between models with and without distant mass clumps.

3.2. Virgo Cluster

The model reveals the maximum or minimum projected infall velocity allowed for a galaxy near the Virgo Cluster along the specified line of sight. *The envelope of velocities provided by our modeling is acutely dependent on the mass of the Virgo Cluster.*

The problem is illustrated by the two panels of Figure 2. The circles show the observed velocities and angular distances from the cluster center of galaxies that are certified to be within the Virgo infall zone on the basis of distance measurements. The small open circles correspond to galaxies projected onto the cluster and, hence, are probable cluster members. The 35 filled circles correspond to galaxies projected outside the Virgo caustic and must be galaxies falling in a quasi-laminar flow into the cluster. The vertical bars bracket maximum and minimum projected velocities in the line of sight of groups of the infalling galaxies for two different models. In the case of the top panel, a model with $M/L = 200\ M_\odot/L_\odot$ assigned to all galaxies and $\Omega_0 = 0.30$ is considered. This model provides a reasonable χ^2 fit for the overall NAM analysis but fails miserably to predict the observed infall velocities. The bottom panel illustrates an example of a good fit for the infall region. In this case, most of the galaxies are now only given $M/L = 150hM_\odot/L_\odot$ in an $\Omega_0 = 0.30$ universe but the Virgo Cluster and 12 other E/S0 knots are given $M/L = 1000h\ M_\odot/L_\odot$. The corresponding mass for Virgo is $1.3 \times 10^{15}\ M_\odot$, higher than the Virial theorem mass of $0.7 \times 10^{15}\ M_\odot$ (Tully & Shaya 1984), but our infall mass pertains to a scale $\sim 3\times$ larger than the Virial radius.

3.3. Local Group

We are presently reworking the analysis of the Local Group, now using 54 mass tracers and including groups out to 6 Mpc to properly provide the tidal field. A typical solution for the trajectories of this system is presented in Figure 3. We have improved the force law softening by distributing the mass of each mass tracer in a halo that grows linear with radius. The rate of growth of mass with

https://doi.org/10.1017/S0252921100055433 Published online by Cambridge University Press

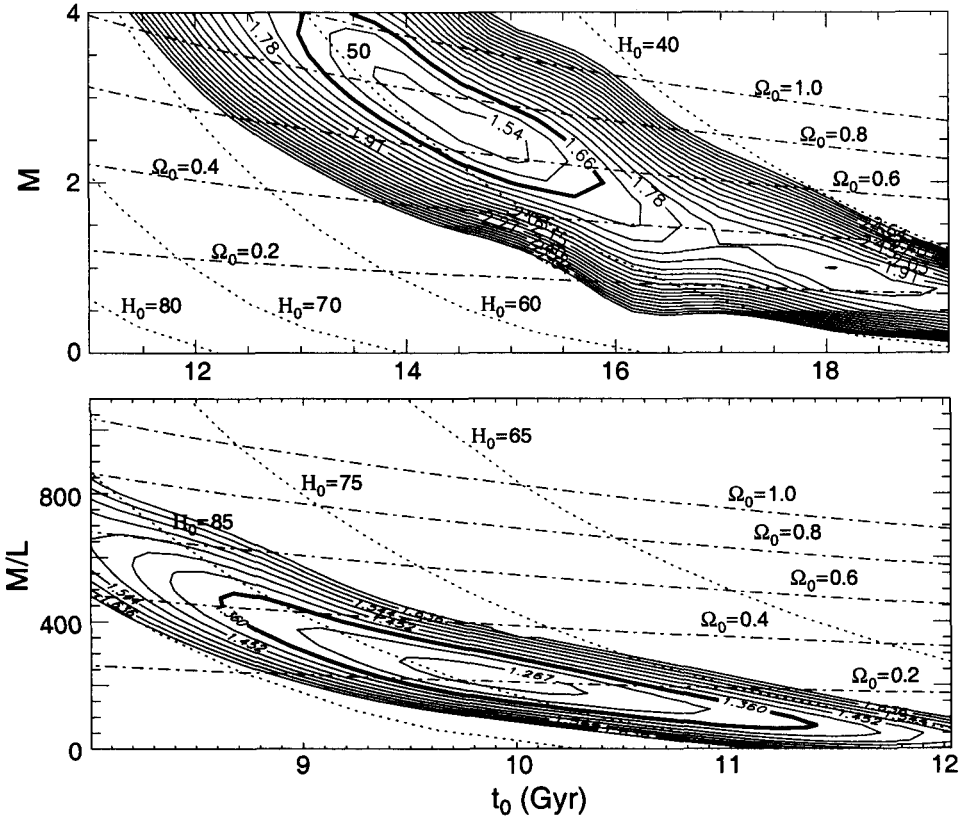

Figure 1. χ^2 map of NAM models as functions of mass and age. Top: CDM N-body simulation with $\Omega_0 = 1$. Bottom: real universe. The HST cepheid distances have resulted in a 15% revision in the distance scale zero-point which does not affect the Ω_0 estimates but which increases the age scale by 15% from that in Fig. 1. Also, a non-zero cosmological constant would increase the ages. The Ω_0 values are to be reinterpreted as the matter fraction of Ω_0.

https://doi.org/10.1017/S0252921100055433 Published online by Cambridge University Press

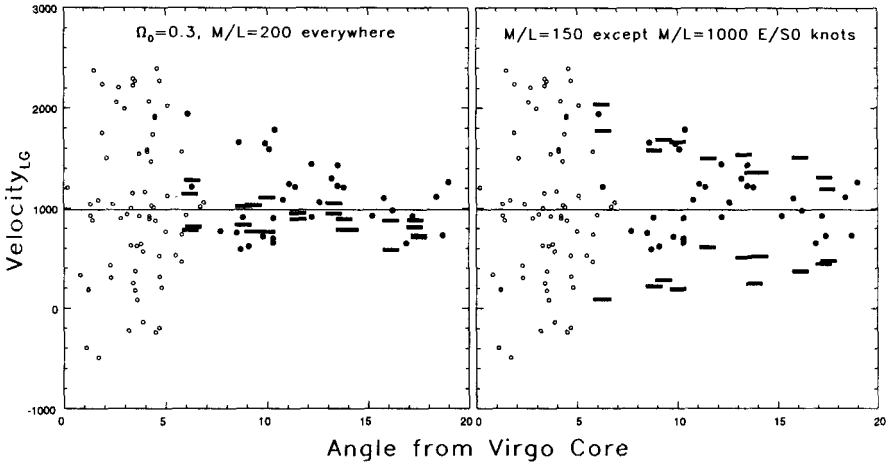

Figure 2. Virgo infall constraints from two models. Vertical bars bracket the line-of-sight extrema velocities for a good global M/L (top) and for a model with a lot of mass in Virgo (bottom).

radius is proportional to the square-root of the luminosity and is normalized by assuming that the Milky Way has a halo radius of 100 kpc when $M/L = 100$. We allow the halo to have collapsed from a maximum radius of twice the present radius at around $z = 1$. Earlier than that it was expanding in proportion to a(t).

Most recently we have been allowing individual masses of mass tracers to float. The procedure is to change the M/L ratio of a mass tracer by 20% in both directions and solve for new orbits. The new mass ($M/1.2$, M, or $1.2\,M$) is set to the one with the lowest of the three χ^2 values. Then the next mass is varied. One loops around all of the mass tracers with significant mass until the χ^2 value levels off. This appears to be a stable way to hunt for possible total mass estimates of galaxies. However, we are not yet ready to report on the outcome.

References

Branchini, E., & Carlberg, R. G. 1994, ApJ, 434, 37

Dunn, A. M., & Laflamme, R. 1993, MNRAS, 264, 865

Dunn, A. M., & Laflamme, R. 1995, ApJ, 443, L1

Kaiser, N. 1984, ApJ284 L9

Lauer, T. R., & Postman, M. 1994, ApJ425 418

Peebles, P. J. E. 1980, in *The Large-Scale Structure of the Universe*, (Princeton: Princeton University Press)

Peebles, P. J. E. 1989, ApJ, 344, L53

https://doi.org/10.1017/S0252921100055433 Published online by Cambridge University Press

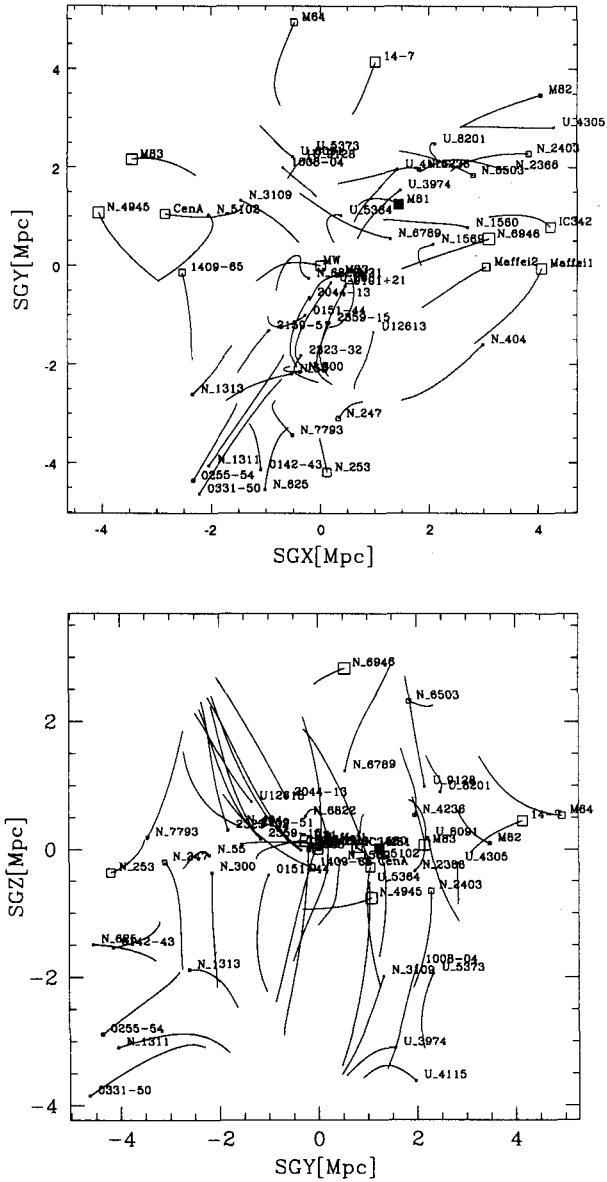

Figure 3. A typical solution for individual galaxies and a few groups within 5 Mpc of the Milky Way. $M/L = 75$, $t_0 = 11$ Gyr, $\Lambda = 0$

https://doi.org/10.1017/S0252921100055433 Published online by Cambridge University Press

Peebles, P. J. E. 1990, ApJ, 362, 1
Peebles, P. J. E. 1994, ApJ, 429, 43
Peebles, P. J. E. 1995, ApJ, 449, 52
Shaya, E. J., Peebles, P. J. E., & Tully, R.B. 1995, ApJ, 454, 15
Shaya, E. J., & Tully, R. B. 1984, ApJ, 281, 56
Shaya, E. J., Tully, R. B., & Pierce, M. J. 1992, ApJ, 391, 16
Tully, R. B. 1988*a*, *Nearby Galaxies Catalog*, (Cambridge: Cambridge University Press)